
A Novel Dataset for Keypoint Detection of Quadruped Animals from Images

Prianka Banik

Department of Computer Science
Prairie View A&M University
pbanik@pvamu.edu

Lin Li

Department of Computer Science
Prairie View A&M University
lilin@pvamu.edu

Xishuang Dong

Department of Electrical and Computer Engineering
Prairie View A&M University
xidong@pvamu.edu

Abstract

In this paper, we studied the problem of localizing a generic set of keypoints across multiple quadruped or four-legged animal species from images. Due to the lack of large scale animal keypoint dataset with ground truth annotations, we developed a novel dataset, AWA Pose, for keypoint detection of quadruped animals from images. Our dataset contains significantly more keypoints per animal and has much more diverse animals than the existing datasets for animal keypoint detection. We benchmarked the dataset with a state-of-the-art deep learning model for different keypoint detection tasks, including both seen and unseen animal cases. Experimental results showed the effectiveness of the dataset. We believe that this dataset will help the computer vision community in the design and evaluation of improved models for the generalized quadruped animal keypoint detection problem.

1 Introduction

Detecting keypoints of quadruped animals has several practical applications in animal behavior understanding [13], automated identification and tracking [20], part segmentation [14], etc. Different quadruped animals vary highly in shapes and they can show wide range of poses. These make the keypoint detection of quadruped animal in wild extremely challenging compared to the intensively studied problem of human keypoint detection from images.

Large scale visual data with manual annotations are required to train the state-of-the-art deep learning based keypoint detection models. However, to the best of our knowledge, there are no large scale datasets of diverse quadruped animal images with corresponding keypoint annotations. Most existing datasets either focus on a single animal or only very few animals [9, 5, 8, 12, 3] or focus on only a very small set of keypoints e.g. facial keypoints [17]. Such datasets are inadequate to train and evaluate large deep learning based models for practical applications. Although quadruped animals have generalized body structures and common body parts, they often come with widely different sizes and shapes. For example, if a dataset contains only known quadruped animals such as dog, cat, horse, cow, sheep, etc. and corresponding keypoints, a model trained with such a dataset may fail to detect the keypoints of new animals like elephant, giraffe, ant-eater, rabbit, kangaroo, etc. Similarly, if a dataset contains large number of animals but only few keypoints such as the facial keypoints, a model trained with such a dataset will have limited usage to only face related applications. Full body

related problems such as 3d model generation, action recognition, and motion analysis cannot be solved with such datasets.

To address this problem, we built a large scale dataset for the quadruped animal keypoint detection problem. The dataset was named AwA Pose as the images were collected from the AwA dataset [22]. To increase the diversity of the images, we included a number of different species in our dataset. By doing so, we ensure that the dataset contains quadruped animals of different sizes and shapes, and therefore, a model trained on the dataset can be applied to unseen quadruped animals. Meanwhile, we also ensure that the animals in the images contains various poses as some animal classes (e.g., cat) can have many different poses which often make keypoint detection very challenging. The images in the dataset contain both self and other forms of occlusions which makes the dataset more generalized. In addition, we proposed a generic set of keypoints for all quadruped animals. The keypoint set includes almost all the body parts of the animals and thus makes the dataset useful for various practical applications.

Besides developing the dataset, we benchmarked it using a state-of-the-art deep learning model for keypoint detection. Experimental results show that the model trained on the dataset can be successfully applied to both seen animals with different poses and novel animals with same and different poses. This ensures that the dataset contains enough diversities to train a generalized keypoint detection model.

Through this work, we intend to give the computer vision research community a new venue to develop and evaluate computer vision models for the quadruped animal keypoint detection problem. The dataset is available to public through github repository <https://github.com/prinik/AwA-Pose>.

2 Related Works

Keypoint detection of objects is a highly studied topic in computer vision. Most of the previous work focused on understanding human keypoints due to its applications in human computer interaction [10], action recognition [6, 11, 25], human pose transfer [15, 26], 3D shape estimation [7, 16], etc. Compared with these efforts, very few had explored the problems of animal keypoint, part or shape estimation from images. Zuffi et. al. [28] explored the problem of novel quadruped animal 3D shape estimation by utilizing 3D scans of toy figurines due to the lack of 3D scan data of real quadruped animals. Some previous research also explored estimating the keypoints of animals using self-supervision approaches [27, 2, 21], but these keypoints are difficult to evaluate as there are no corresponding ground truth data. Some previous work limited the problem to only facial keypoint detection from animal images [17, 24]. Recently, Cao et al [4] combined the keypoint annotation of human and quadruped animals to train a deep learning model which showed superior performance for the whole body keypoint estimation problem of novel quadruped animals. But they did not provide any quantitative results on novel quadruped animals due to the lack of existing large scale dataset of quadruped animals with keypoint annotations. Also, many animals have unique keypoints which are missing in human beings (e.g., tail end and horns). Moreover, their seen and unseen animals are pretty similar in shapes. It is not clear how well their approach will perform for animals with unusual body features (e.g., giraffe—long neck, elephant—trunk, etc.)

The need for a large scale quadruped animal keypoint dataset becomes more evident when the state-of-the-art deep learning models for keypoint detection such as HRNet [19] are used. Such models requires large number of annotated data for training. Also, without a proper testing dataset, it is difficult to understand the performance improvements of the new models. Existing datasets such as Animal Pose [3] have few body keypoints for only five species of quadruped animals. The sparse keypoints are not very useful for problems such as 3D shape reconstructions. All these drove us to create a large scale quadruped animal keypoint dataset with diverse animals and a large number of keypoints.

3 Our Dataset

The goal of this paper is to introduce a new large scale dataset of quadruped animal keypoint—AwA Pose. We built the dataset using images from the AwA [22] dataset. AwA contains images of 50 animal species from which we selected 35 quadruped animal species. Compared with the existing animal keypoint datasets, AwA Pose better facilitates the training and testing of deep learning models

Dataset	Images	Species	Keypoints
Animal Pose [3]	3608	5	20
Horse-10 [12]	8114	1	22
MacaquePose [8]	13083	1	17
Grévy’s Zebra [5]	900	1	9
ATRW [9]	8076	1	15
AwA Pose (Our Dataset)	10064	35	39

Table 1: List of selected generic keypoint datasets for the quadruped animals.

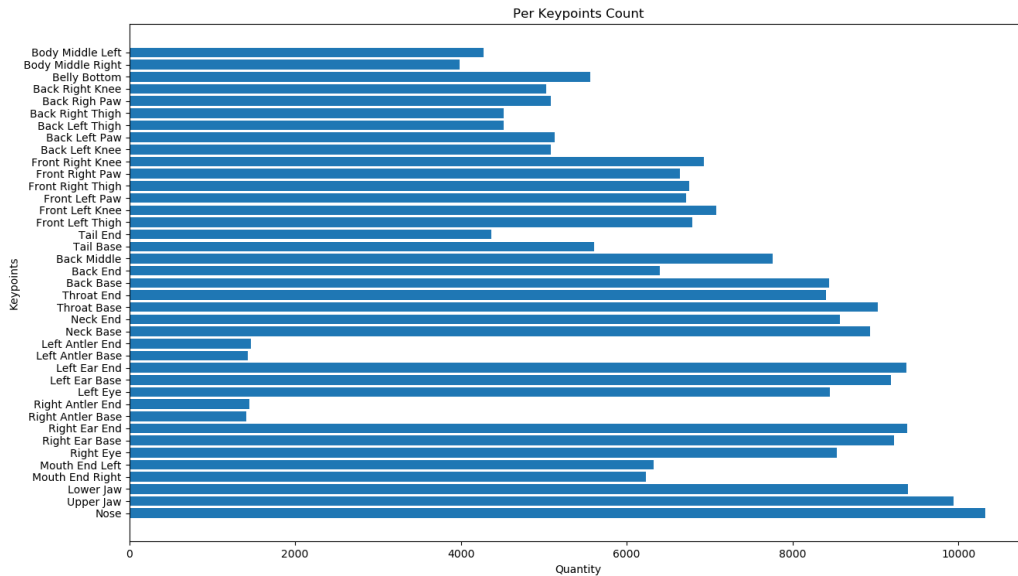


Figure 1: Number of images per keypoint.

with both more animals species and higher number of keypoints. For example, Animal Pose [3] contains five animal species which is higher than the other datasets but still much lower than the number of animal species covered by our dataset. On the other hand, Horse-10 [12] has the largest set of keypoints after ours, but it only contains a single animal ‘Horse’ and the number of keypoints is much smaller than AwA Pose. The MacaquePose [8] dataset contains the most number of images (13k) where our dataset contains a comparable number of images (10k) and much more animals and keypoints. A detailed comparison of the datasets is shown in Table 1. In the following sections, we will discuss in details about the keypoint set and the annotation process.

3.1 Keypoint Set

We first fixed a generic set of keypoints for all the selected quadruped animals. While most of the existing datasets only provide annotation for a very small number of keypoints, our dataset provides a much larger number of keypoints for better understanding the animal’s poses. Our goal is to annotate as many keypoints as possible so we can cover almost all the body parts of the animal. This will help applications which requires dense keypoints such as 3D reconstruction, pose estimation, etc. The keypoints we adopted are mostly from Animal Pose [3]. We augmented the keypoints by adding more details such as ‘Tail End’, ‘Mouth End Left’, ‘Mouth End Right’, etc. A list of the 39 keypoints and their corresponding numbers of images is shown in Figure 1. It should be noted that we only annotated the visible keypoints in a specific picture. Figure 1 shows that the upper body keypoints and facial keypoints are visible in most of the images. Keypoints related to the body part ‘Antler’ are most rare as only few animals have ‘Antler’. Other than ‘Antler’, all other keypoints have around 4k annotated images.

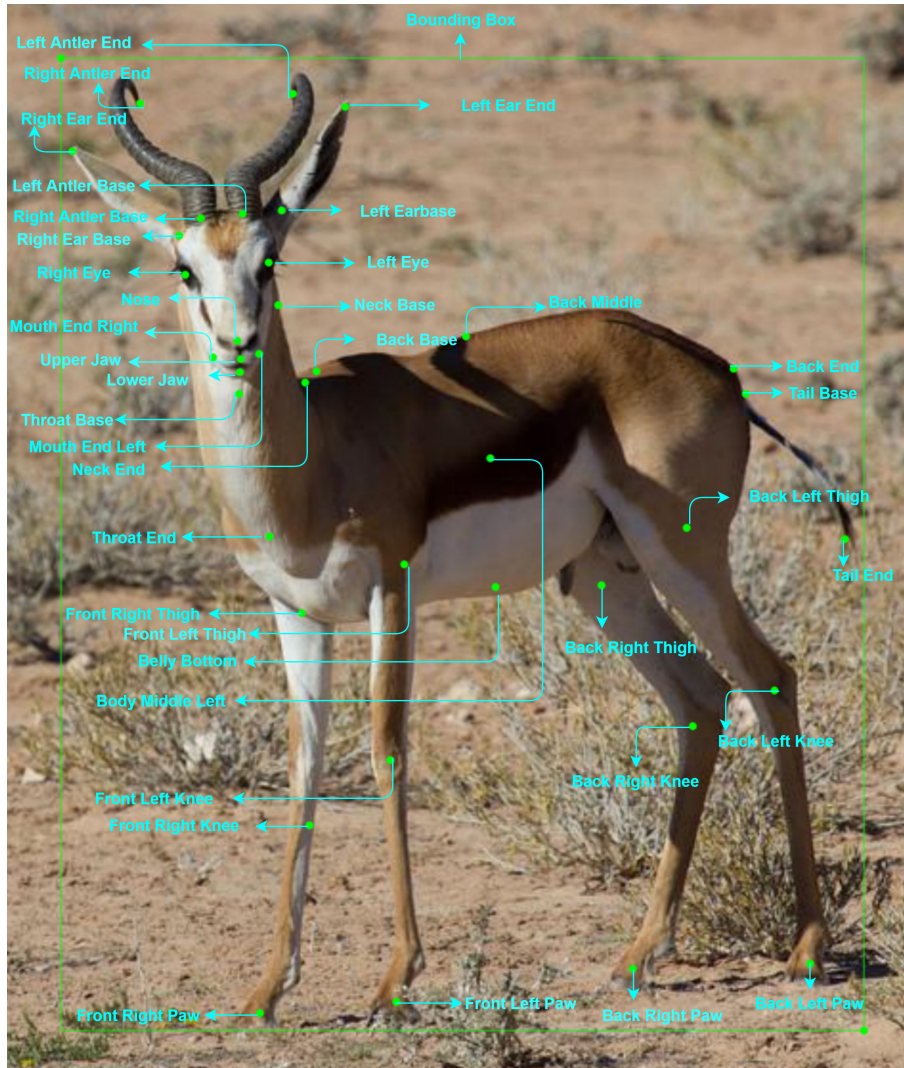


Figure 2: Example annotation of a quadruped animal with keypoints and bounding box.

3.2 Annotation

After selecting the list of the keypoints, we selected images of 35 quadruped animal classes from the AwA dataset. For the current AwA Pose dataset, we only included the images where there is a single animal presenting. In the future, we plan to include multiple instance images to expand dataset. To annotate the keypoints and the bounding box of the animal in each image, we used the LabelMe [18] tool. A sample annotation is shown in Figure 2. As depicted, our keypoint set covers a lot of details of the animal body so they can be useful for various applications such as fine grained action recognition, part segmentation, and 3D reconstruction. Per image annotation took around 5 minutes. We also tried to annotate roughly the same number of images for each animal class to make the dataset balanced. The number of annotated images per animal class can be seen in Figure 3. In total, we have annotated around 10k images with keypoint and bounding box annotations.

3.3 Model for Dataset Evaluation

We have trained the HRNet [23] model for detecting the keypoints from the quadruped animal images using our keypoint annotations. HRNet [23] has shown superior performances for human keypoint detection problem thus should be suitable benchmarking model for our animal keypoint dataset. The HRNet [23] model is a convolutional neural network model which can keep the 2D feature resolution

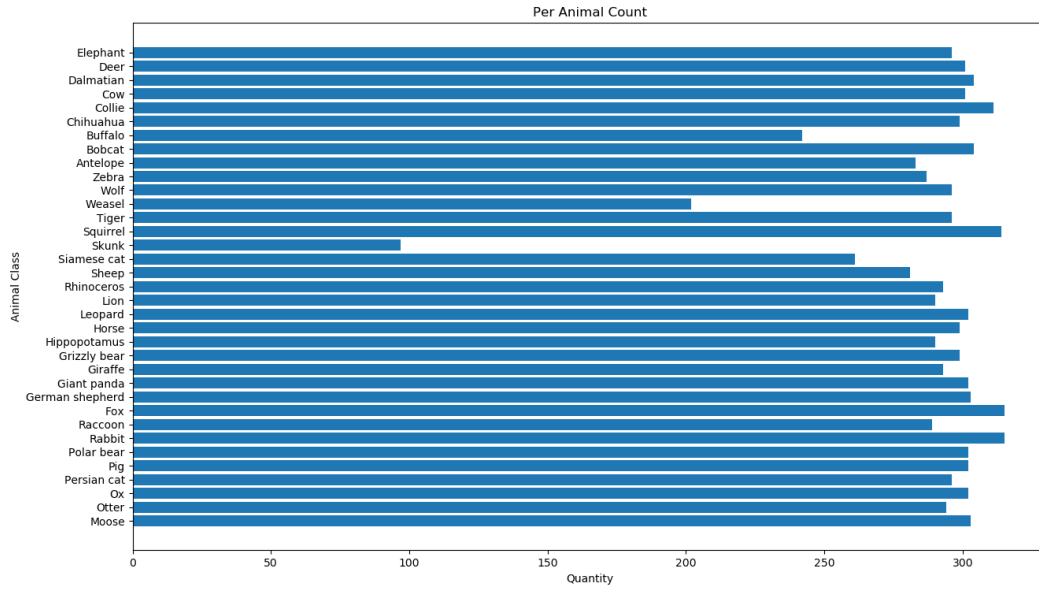


Figure 3: Number of images per animal class.

high throughout the whole network. It has multiple scale streams where the topmost stream keeps the convolutional feature resolution same as the input image which helps to detect keypoints even when the animal body part is very small (e.g., eyes, nose tip, etc.) But large convolutional feature maps cannot learn global information due to the small convolution kernel size and large feature map size which are only suitable for learning local information (e.g., only eye or nose). To accurately detect each of the keypoints, it is important to have a global knowledge of all the keypoints locations. This will provide contextual information for detecting occluded and ambiguous keypoints. For example, if the ‘back left paw’ keypoint is occluded by grass and the keypoint ‘back left knee’ is clearly visible, the location of ‘back left knee’ can help detect the keypoint ‘back left paw’. HRNet also downscale the feature size to various scales (e.g., 2x, 4x) and then uses skip-connections to upscale and feed them back to the original high resolution stream. This overall approach allows the network to detect keypoints efficiently from images even in difficult cases. The HRNet model generates heatmaps for each of the keypoints in our predefined keypoint dictionary. The center of the keypoints are considered as the predicted 2D locations of the keypoints. As the images of our current dataset only contain a single animal, we did not use the annotated bounding boxes for training although they were used for evaluation.

4 Experiments and Analysis

To evaluate the HRNet for detecting keypoints on our quadruped animal keypoint dataset, we conducted several experiments for both seen and unseen animals. For each of the experiments, we examined the model performance for each individual keypoints.

4.1 Training

In this research, the HRNet-W48 version of the HRNet model was trained for our experiments. We used input image resolution 384x288 and output heatmap resolution 96x72. During the training time, we used data augmentations such as mirroring, rotating and scaling of both the training images and corresponding keypoint annotations. The minibatch size is 20 and the initial learning rate is 5e-4. Also, we used Adam optimizer for the training and trained the model for 120 epochs. For both the seen and unseen animal keypoint detection experiments, 5-fold cross validation was used. For the seen animal experiments, we randomly chose around 20 images per animal for testing. We selected roughly full body animal images for testing to use the bounding box as the scale for the animal for evaluation. For the unseen animal experiment, we randomly chose four animals for testing and the

keypoint	Seen Animals			Unseen Animals		
	@0.001	@0.0005	@0.0001	@0.001	@0.0005	@0.0001
Nose	0.99	0.88	0.42	0.98	0.85	0.39
Upper Jaw	0.99	0.88	0.45	0.96	0.83	0.4
Lower Jaw	0.97	0.83	0.38	0.94	0.77	0.35
Mouth End Right	0.97	0.79	0.34	0.94	0.71	0.27
Mouth End Left	0.97	0.79	0.33	0.94	0.71	0.26
Right Eye	0.99	0.91	0.55	0.98	0.88	0.51
Right Ear Base	0.97	0.79	0.3	0.96	0.76	0.29
Right Ear End	0.96	0.83	0.41	0.93	0.79	0.4
Right Antler Base	0.97	0.74	0.3	0.93	0.73	0.22
Right Antler End	0.88	0.68	0.37	0.73	0.57	0.23
Left Eye	0.99	0.92	0.54	0.98	0.89	0.53
Left Ear Base	0.98	0.8	0.32	0.96	0.76	0.28
Left Ear End	0.95	0.82	0.41	0.92	0.79	0.41
Left Antler Base	0.97	0.79	0.34	0.96	0.8	0.29
Left Antler End	0.89	0.75	0.47	0.85	0.67	0.26
Neck Base	0.9	0.64	0.2	0.87	0.57	0.18
Neck End	0.84	0.54	0.16	0.78	0.49	0.15
Throat Base	0.93	0.64	0.21	0.87	0.59	0.16
Throat End	0.85	0.53	0.15	0.81	0.47	0.13
Back Base	0.82	0.5	0.14	0.78	0.47	0.13
Back End	0.73	0.44	0.14	0.68	0.4	0.12
Back Middle	0.73	0.45	0.14	0.68	0.4	0.12
Tail Base	0.75	0.46	0.13	0.72	0.45	0.13
Tail End	0.74	0.51	0.17	0.7	0.49	0.17
Front Left Thigh	0.8	0.44	0.12	0.79	0.42	0.11
Front Left Knee	0.82	0.49	0.14	0.8	0.46	0.12
Front Left Paw	0.88	0.62	0.19	0.87	0.61	0.18
Front Right Thigh	0.81	0.44	0.13	0.8	0.42	0.11
Front Right Paw	0.88	0.61	0.18	0.89	0.59	0.18
Front Right Knee	0.82	0.5	0.12	0.83	0.47	0.12
Back Left Knee	0.76	0.42	0.13	0.69	0.37	0.11
Back Left Paw	0.83	0.55	0.17	0.82	0.52	0.17
Back Left Thigh	0.73	0.38	0.11	0.68	0.32	0.09
Back Right Thigh	0.74	0.37	0.11	0.69	0.35	0.1
Back Right Paw	0.84	0.57	0.17	0.81	0.54	0.15
Back Right Knee	0.76	0.42	0.12	0.73	0.37	0.1
Belly Bottom	0.85	0.55	0.17	0.82	0.51	0.13
Body Middle Right	0.69	0.33	0.1	0.66	0.3	0.09
Body Middle Left	0.71	0.34	0.11	0.65	0.3	0.08
Avg	0.86	0.61	0.24	0.83	0.57	0.21

Table 2: PCKB results for the seen and unseen animals for HRNet.

rest of the animals for training. Thus during training time, none of the animals in the test dataset are seen by the model. We conducted this experiment to see if a model can learn the generalized concept of the keypoints from our dataset. Experimental results indicate that our dataset is particularly suitable for such applications as AWA Pose contains 35 different quadruped animals.

4.2 Evaluation Criteria

To evaluate the model’s performance on our dataset, we used the widely adopted metric, PCK (Percentage of Correct Key-points) [1]. PCK considers a keypoint detection correct if the detection is within a given threshold. As the quadruped animals can vary widely in shapes and sizes, we used the bounding box annotations for the animals to calculate the threshold. We consider the keypoint detection correct, if the distance between the predicted keypoint location and the ground

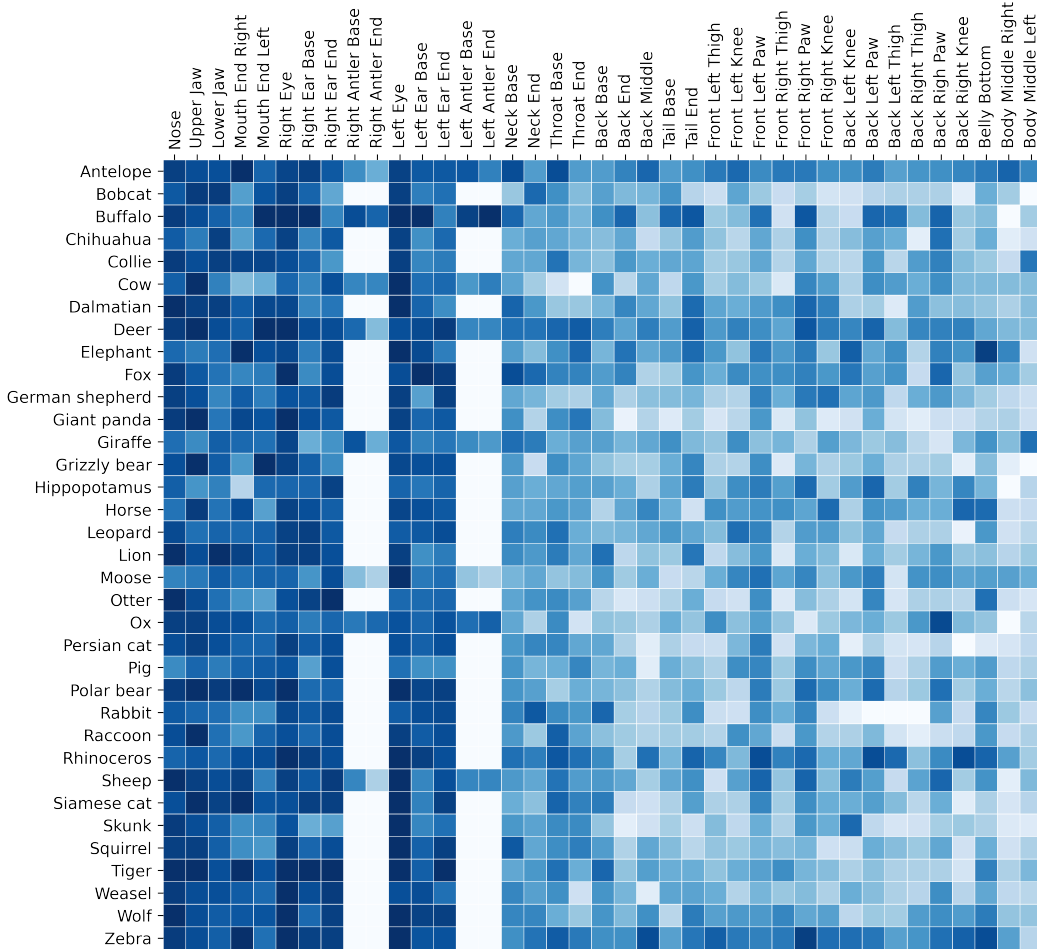


Figure 4: Per keypoint PCKB@0.0005 for each animal for the seem animal experiment. Dark blue indicates higher PCKB where lighter blue indicates lower PCKB.

truth keypoint detection is within a certain value multiplied by the diagonal of the animal bounding box. This way, the evaluation is independent of the animal size. We named the evaluation criteria PCKB with B referring to the "bounding box". The calculation of PCKB is as follows:

$$PCKB = \frac{1}{K} \sum_{i=1}^K \mathbb{I}[dist_i < SF * D] \quad (1)$$

where $dist_i$ is the distance between the predicted and the ground truth locations of the i th keypoint; D is the length of the diagonal of the bounding box; SF is a scale factor for deciding the distance threshold in terms of D (e.g., $PCKB@0.001$ is the PCKB value while $SD = 0.001$); K is the total number of visible keypoints; \mathbb{I} is an indicator function which produces one if the condition is true, otherwise zero. PCKB is ranged between 0 to 1 and higher PCKB indicates higher detection accuracy.

4.3 Results for Seen Animals

Table 2 presents the results of the seen animal experiments in which we used three different scale factors for the distance threshold calculation, 0.001, 0.0005, and 0.0001. The bigger the value, the more the tolerance is given while measuring correctness of the predicted keypoint location. Accordingly, we get higher PCKB values for larger multipliers and lower PCKB values for smaller multipliers. This also indicates the efficacy of our evaluation criteria, as lower distance threshold

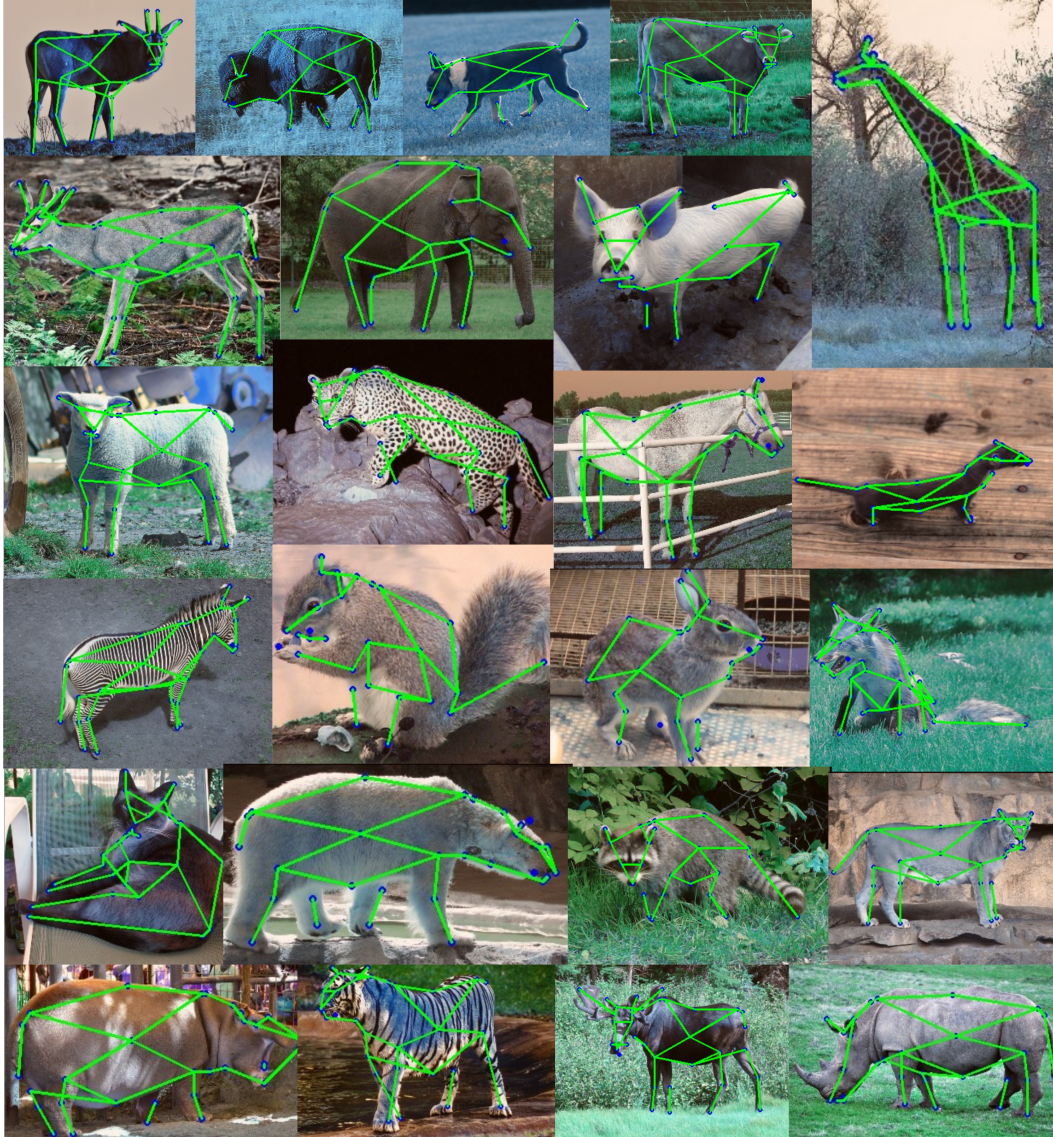


Figure 5: Qualitative results of the seen animal experiment.

is making it stricter to pass a prediction as a success while higher distance threshold is making it comparatively easier. The results also show that the PCKB for the upper body keypoints such as the facial keypoints are much higher than the lower body keypoints. This is probably due to the complex and articulated poses presented by the lower body parts (e.g., legs), which is illustrated in Figure 4. A PCKB value was calculated for each pair of animal species and keypoint type. Darker blue indicates higher PCKB value and lighter blue indicates lower PCKB values. It can be clearly seen that the left part of the heatmap shows the higher values which represents the upper body keypoints and the right part of the heatmap shows lower PCKB values which represents mostly the lower body keypoints. Also, we can see that for most animals, the lowest body keypoints (i.e., paws) are well detected. But for small animals, such as rabbit, squirrel, and skunk, the lower body parts are more difficult to detect. On the other hand, some big animals such as giant panda can be difficult too as it's smaller body parts can be occluded by larger body parts. Moreover, for animals which often present complex poses, such as persian cat and siamese cat, it can be very difficult to detect the lower body parts. But overall, the model can localize the keypoints pretty well as shown in Figure 5. Figure 6 depicts some failure cases. In general, if the body parts are over occluded or the viewing angle is very different (e.g., top view), the model performance is poor.



Figure 6: Failure cases for the seen experiment.

4.4 Results for Unseen Animals

We also conducted experiments for unseen animal keypoint detection where the model was trained on some animal species and then applied to a completely different set of animal species. The results are shown in Table 2. As we can see, the results for the zero-shot experiment are similar to the seen experiments. Although the PCKB values for the unseen animals are always lower than those of the seen animals, they are very close. This indicates that a model trained using our dataset can be generalized to unseen quadruped animals. This is due to the inclusion of diverse quadruped animals and dense keypoints in our dataset.

5 Conclusion

In this paper, we introduce a novel quadruped animal keypoint dataset—AwA Pose in which we annotated a large number of images with dense keypoints. Our dataset contains 35 different animal species and a total of 39 different keypoints. Both numbers are much higher than those of the existing datasets. Experimental results show that the dataset can be applied to both seen and unseen animal keypoint detection with solid performance. As detecting animal keypoints is significantly harder than human keypoints due to the animals' wide variance in sizes and shapes, we believe that our dataset will contribute to the computer vision community by reducing the gap between human and animal keypoint detection research. The dataset can be used as a test bed for novel keypoint detection models. It can also be used for more downstream tasks such as action recognition, part segmentation, 3D reconstruction, etc.

References

- [1] Mykhaylo Andriluka, Leonid Pishchulin, Peter Gehler, and Bernt Schiele. 2d human pose estimation: New benchmark and state of the art analysis. In *Proceedings of the IEEE Conference on computer Vision and Pattern Recognition*, pages 3686–3693, 2014.

- [2] Anatoly Belikov and Alexey Potapov. Goodpoint: unsupervised learning of keypoint detection and description. *arXiv preprint arXiv:2006.01030*, 2020.
- [3] Jinkun Cao, Hongyang Tang, Hao-Shu Fang, Xiaoyong Shen, Cewu Lu, and Yu-Wing Tai. Cross-domain adaptation for animal pose estimation. In *The IEEE International Conference on Computer Vision (ICCV)*, October 2019.
- [4] Jinkun Cao, Hongyang Tang, Hao-Shu Fang, Xiaoyong Shen, Cewu Lu, and Yu-Wing Tai. Cross-domain adaptation for animal pose estimation. In *Proceedings of the IEEE/CVF International Conference on Computer Vision*, pages 9498–9507, 2019.
- [5] Jacob M Graving, Daniel Chae, Hemal Naik, Liang Li, Benjamin Koger, Blair R Costelloe, and Iain D Couzin. Fast and robust animal pose estimation. *bioRxiv*, page 620245, 2019.
- [6] Michael B Holte, Cuong Tran, Mohan M Trivedi, and Thomas B Moeslund. Human pose estimation and activity recognition from multi-view videos: Comparative explorations of recent developments. *IEEE Journal of selected topics in signal processing*, 6(5):538–552, 2012.
- [7] Muhammed Kocabas, Nikos Athanasiou, and Michael J Black. Vibe: Video inference for human body pose and shape estimation. In *Proceedings of the IEEE/CVF Conference on Computer Vision and Pattern Recognition*, pages 5253–5263, 2020.
- [8] Rollyn Labuguen, Jumpei Matsumoto, Salvador Blanco Negrete, Hiroshi Nishimaru, Hisao Nishijo, Masahiko Takada, Yasuhiro Go, Ken-ichi Inoue, and Tomohiro Shibata. Macaquepose: A novel “in the wild” macaque monkey pose dataset for markerless motion capture. *Frontiers in behavioral neuroscience*, 14, 2020.
- [9] Shuyuan Li, Jianguo Li, Hanlin Tang, Rui Qian, and Weiyao Lin. Atrw: a benchmark for amur tiger re-identification in the wild. *arXiv preprint arXiv:1906.05586*, 2019.
- [10] Hai Liu, Hanwen Nie, Zhaoli Zhang, and You-Fu Li. Anisotropic angle distribution learning for head pose estimation and attention understanding in human-computer interaction. *Neurocomputing*, 433:310–322, 2021.
- [11] Diogo C Luvizon, David Picard, and Hedi Tabia. 2d/3d pose estimation and action recognition using multi-task deep learning. In *Proceedings of the IEEE Conference on Computer Vision and Pattern Recognition*, pages 5137–5146, 2018.
- [12] Alexander Mathis, Thomas Biasi, Steffen Schneider, Mert Yuksekogonul, Byron Rogers, Matthias Bethge, and Mackenzie W Mathis. Pretraining boosts out-of-domain robustness for pose estimation. In *Proceedings of the IEEE/CVF Winter Conference on Applications of Computer Vision*, pages 1859–1868, 2021.
- [13] Mackenzie Weygandt Mathis and Alexander Mathis. Deep learning tools for the measurement of animal behavior in neuroscience. *Current opinion in neurobiology*, 60:1–11, 2020.
- [14] Shujon Naha, Qingyang Xiao, Prianka Banik, Md. Alimoor Reza, and David J. Crandall. Part segmentation of unseen objects using keypoint guidance. In *Proceedings of the IEEE/CVF Winter Conference on Applications of Computer Vision (WACV)*, pages 1742–1750, January 2021.
- [15] Natalia Neverova, Riza Alp Guler, and Iasonas Kokkinos. Dense pose transfer. In *Proceedings of the European conference on computer vision (ECCV)*, pages 123–138, 2018.
- [16] Mohamed Omran, Christoph Lassner, Gerard Pons-Moll, Peter Gehler, and Bernt Schiele. Neural body fitting: Unifying deep learning and model based human pose and shape estimation. In *2018 international conference on 3D vision (3DV)*, pages 484–494. IEEE, 2018.
- [17] Maheen Rashid, Xiuye Gu, and Yong Jae Lee. Interspecies knowledge transfer for facial keypoint detection. In *Proceedings of the IEEE Conference on Computer Vision and Pattern Recognition*, pages 6894–6903, 2017.
- [18] BryanC. Russell, Antonio Torralba, KevinP. Murphy, and WilliamT. Freeman. Labelme: A database and web-based tool for image annotation. *International Journal of Computer Vision*, 77(1-3):157–173, 2008.
- [19] Ke Sun, Bin Xiao, Dong Liu, and Jingdong Wang. Deep high-resolution representation learning for human pose estimation. In *Proceedings of the IEEE/CVF Conference on Computer Vision and Pattern Recognition*, pages 5693–5703, 2019.
- [20] Eric T Psota, Ty Schmidt, Benny Mote, and Lance C Pérez. Long-term tracking of group-housed livestock using keypoint detection and map estimation for individual animal identification. *Sensors*, 20(13):3670, 2020.
- [21] James Thewlis, Hakan Bilen, and Andrea Vedaldi. Unsupervised learning of object landmarks by factorized spatial embeddings. In *Proceedings of the IEEE international conference on computer vision*, pages 5916–5925, 2017.
- [22] Yongqin Xian, Christoph H Lampert, Bernt Schiele, and Zeynep Akata. Zero-shot learning—a comprehensive evaluation of the good, the bad and the ugly. *IEEE transactions on pattern analysis and machine intelligence*, 41(9):2251–2265, 2018.
- [23] Bin Xiao, Haiping Wu, and Yichen Wei. Simple baselines for human pose estimation and tracking. In *European Conference on Computer Vision (ECCV)*, 2018.
- [24] Heng Yang, Renqiao Zhang, and Peter Robinson. Human and sheep facial landmarks localisation by triplet interpolated features. In *2016 IEEE Winter Conference on Applications of Computer Vision (WACV)*, pages 1–8. IEEE, 2016.

- [25] Angela Yao, Juergen Gall, Gabriele Fanelli, and Luc Van Gool. Does human action recognition benefit from pose estimation?". In *Proceedings of the 22nd British machine vision conference-BMVC 2011*. BMV press, 2011.
- [26] Mihai Zanfir, Alin-Ionut Popa, Andrei Zanfir, and Cristian Sminchisescu. Human appearance transfer. In *Proceedings of the IEEE Conference on Computer Vision and Pattern Recognition*, pages 5391–5399, 2018.
- [27] Yuting Zhang, Yijie Guo, Yixin Jin, Yijun Luo, Zhiyuan He, and Honglak Lee. Unsupervised discovery of object landmarks as structural representations. In *Proceedings of the IEEE Conference on Computer Vision and Pattern Recognition*, pages 2694–2703, 2018.
- [28] Silvia Zuffi, Angjoo Kanazawa, David W Jacobs, and Michael J Black. 3d menagerie: Modeling the 3d shape and pose of animals. In *Proceedings of the IEEE conference on computer vision and pattern recognition*, pages 6365–6373, 2017.